Global Fits of the CKM Matrix

G. Eigen¹ G.P. Dubois-Felsmann², D.G. Hitlin², and F.C. Porter²

- ¹ Dept. of Physics, University of Bergen
- ² Lauritsen Laboratory, Caltech

the date of receipt and acceptance should be inserted later

Abstract. We report upon the present status of global fits to Cabibbo-Kobayashi-Maskawa matrix.

PACS. XX.XX.XX No PACS code given

1 Introduction

The three-family Cabibbo-Kobayashi-Maskawa (CKM) quark-mixing matrix is a key element of the Standard Model (SM). The nine complex CKM elements are completely specified by three mixing angles and one phase that is responsible for CP violation in the SM. Measuring the CKM matrix elements in various ways provides consistency tests of the matrix elements itself and with unitarity. Any significant inconsistency with the SM would indicate the presence of new physics.

A convenient parameterization of the CKM matrix is the Wolfenstein approximation [1], which to order $O(\lambda^3)$ is given by:

$$V = \begin{pmatrix} 1 - \frac{\lambda^2}{2} & \lambda & A\lambda^3(\rho - i\eta) \\ -\lambda & 1 - \frac{\lambda^2}{2} & A\lambda^2 \\ A\lambda^3(1 - \bar{\rho} - i\bar{\eta}) & -A\lambda^2 & 1 \end{pmatrix} + O(\lambda^4),$$
(1)

where $\lambda=0.2241\pm0.0033$ is the best-known parameter measured in semileptonic K decays, A=0.82 is determined from semileptonic B decays to charmed particles with an accuracy of $\simeq 6\%$ and $\bar{\rho}=\rho\cdot(1-\lambda^2/2)$ and $\bar{\eta}=\eta\cdot(1-\lambda^2/2)$ are least-known.

The unitarity of the CKM matrix yields six triangular relations of which $V_{ud}V_{ub}^* + V_{cd}V_{cb}^* + V_{td}V_{tb}^* = 0$ is well-suited for experimental tests. In order to determine the apex of the unitarity triangle $(\bar{\rho}, \bar{\eta})$ presently eight measurements are used as input, the B semileptonic branching fractions $\mathcal{B}(B \to X_c \ell \nu)$, $\mathcal{B}(B \to X_u \ell \nu)$, and $\mathcal{B}(B \to \rho \ell \nu)$, the normalized $B \to D^* \ell \nu$ rate at zero recoil, $\mathcal{F}(1)|V_{ub}|^2$, the B_d^0 and B_s^0 oscillations frequencies Δm_{B_d} and Δm_{B_s} , the parameter $|\epsilon_K|$ that specifies CP violation in the $K^0 \bar{K}^0$ system, as well as $\sin 2\beta$ which is measured in CP asymmetries of charmonium K_S^0 (K_L^0) final states. Though many of these measurements themselves are rather precise their translation to the $\bar{\rho} - \bar{\eta}$ plane is affected by large non-gaussian theoretical uncertainties. Various approaches, which treat theoretical errors in different ways, can be found in the literature [2,3,4,5,6].

2 The Scan Method

The scan method is an unbiased procedure for extracting $A, \bar{\rho}, \bar{\eta}$ from measurements. We select observables that allow us to factorize their predictions in terms of theoretical quantities T_i that have an a priori unknown (and likely non-gaussian) error distribution (Δ_i) , other observables, and the CKM dependence expressed as functions of Wolfenstein parameters. As an example, consider the charmless semileptonic branching fraction for $B \to \rho \ell \nu$, which is predicted to be $\mathcal{B}(B \to \rho \ell \nu) = |V_{ub}|^2 \cdot \widetilde{\Gamma}_{\rho \ell \nu} \cdot \tau_B$, where τ_{B^0} is the B^0 lifetime and $\widetilde{\Gamma}_{\rho \ell \nu}$ is the reduced rate affected by non-gaussian uncertainties. This analysis treats eleven theoretical parameters with non-gaussian errors, the reduced inclusive semileptonic rates $\widetilde{\Gamma}_{X_u\ell\nu}$ and $\widetilde{\Gamma}_{X_c\ell\nu}$, the form factor for $B \to D^*\ell\nu$ at zero recoil, $\mathcal{F}_{D^*}(1)$, the bag factors of the K^0 and B^0 systems, B_K and B_B , the B^0 decay constant f_B , $\xi^2 = f_{B_s}^2/f_{B_d}^2 B_{B_s}/B_{B_d}$ and the QCD parameters η_1, η_2, η_3 and η_B .

We perform a χ^2 minimization based on a frequentist approach by selecting a specific value for each T_i within the allowed range (called a model). We perform individual fits for many models scanning over the allowed nongaussian ranges of the T_i parameter space. The QCD parameters are not scanned; their small errors are treated in the χ^2 as gaussian. For theoretical quantities calculated on the lattice, which have gaussian errors $(B_K, B_B, f_B \text{ and } \xi)$ we add specific χ^2 terms. To account for correlations between observables that occur in more than one prediction, such as the masses of the t-quark, c-quark, and W-boson, B hadron lifetimes, B hadron production fractions and λ , we include additional terms in the χ^2 function.

We consider a model to be consistent with the data if the fit probability yields $P(\chi^2) > 5\%$. We determine the best estimate for each of the 17 fit parameters and plot a 95% confidence level (C.L.) contour in the $\bar{\rho} - \bar{\eta}$ plane. We overlay the $\bar{\rho} - \bar{\eta}$ contours of all accepted fits. In order to study correlations among the T_i and constraints the data impose we perform global fits with non-gaussian theory errors scanned over a $\pm 5\Delta$ wide range (see section 5).

Table 1. Measurement inputs used in χ^2 minimization

Observable	Value	Comment
$\begin{array}{c} \mathcal{B}(B \to X_u \ell \nu) \\ \mathcal{B}(B \to X_u \ell \nu) \\ \mathcal{B}(B \to X_c \ell \nu) \\ \mathcal{B}(B \to X_c \ell \nu) \\ \mathcal{B}(B \to \rho \ell \nu) \\ V_{cb} F(1) \end{array}$	$(2.03 \pm 0.22_{exp} \pm 0.31_{th}) \times 10^{-3}$ $(1.71 \pm 0.48_{exp} \pm 0.21_{th}) \times 10^{-3}$ 0.1070 ± 0.0028 0.1042 ± 0.0026 $(2.68 \pm 0.43_{exp} \pm 0.5_{th}) \times 10^{-3}$ $0.0388 \pm 0.005 \pm 0.009$	$\Upsilon(4S)$ LEP $\Upsilon(4S)$ LEP CLEO/ $BABAR$ LEP/CLEO/ Bel
$ \Delta m_{B_d} \Delta m_{B_s} \epsilon_K \sin 2\beta \lambda $	$(0.503 \pm 0.006) \text{ps}^{-1}$ > 14.4 ps^{-1} @95%C.L. $(2.271 \pm 0.017) \times 10^{-3}$ 0.731 ± 0.055 0.2241 ± 0.0033	world average LEP PDG 2000 [7] BABAR/Belle world average

Table 2. Theoretical parameter with non-gaussian errors

$0.87 \le \mathcal{F}_{D^*}(1) \le 0.95$	$38.0 \le \widetilde{\Gamma}(c\ell\nu) \le 41.5 \text{ ps}^{-1}$
$12.0 \le \widetilde{\Gamma}(\rho\ell\nu) \le 22.2 \text{ ps}^{-1}$	$54.8 \le \widetilde{\Gamma}(u\ell\nu) \le 79.6 \text{ ps}^{-1}$
$0.72 \le B_K \le 1.0$	$\sigma_{B_K} = 0.06 \text{ (gaussian)}$
$211 \le f_{B_d} \sqrt{B_{B_d}} \le 235 \text{ MeV}$	$\sigma_{f_B\sqrt{B_B}} = 33 \text{ MeV (gaussian)}$
$1.18 \le \xi \le 1.30$	$\sigma_{\xi} = 0.04 \text{ (gaussian)}$
$0.54 \le \eta_B \le 0.56$	$1.0 \le \eta_1 \le 1.64$
$0.564 \le \eta_2 \le 0.584$	$0.43 \le \eta_3 \le 0.51$

2.1 Treatment of Δm_{B_s}

Since $B_s^0 \bar{B}_s^0$ oscillations have not been observed yet, a lower limit on Δm_{B_S} at 95% C.L. has been determined by combining analyses of different experiments using the amplitude method [8]. To incorporate Δm_{B_S} into the χ^2 function, we use a new approach that is based upon the significance of a Δm_{B_s} measurement [9]:

$$S = \sqrt{\frac{N}{2}} f_{B_s} (1 - 2w) e^{-\frac{1}{2}(\Delta m_s \sigma_t)^2},$$
 (2)

where N is the sample size, f_{B_s} is the B_s purity, w is the mistag fraction, and σ_t is the resolution. Substituting C for $\sqrt{\frac{N}{2}}f_{B_s}(1-2w)$ and interpreting S as the number of standard deviations by which Δm_{B_s} differs from zero, $S = \Delta m_{B_s}/\sigma_{\Delta m_{B_s}}$, we may define a contribution to the χ^2 from the Δm_{B_s} measurements as:

$$\chi^2_{\Delta m_{B_s}} = C^2 \left(1 - \frac{\Delta}{\Delta m_{B_s}} \right)^2 e^{-(\Delta m_{B_s} \sigma_t)^2},$$
 (3)

where Δ is the best estimate according to experiment. The values of (Δ, C^2, σ_t) are chosen to give a minimum at 17 ps⁻¹, and a $P(\chi^2)=5\%$ at $\Delta m_{B_s}=14.4$ ps⁻¹. In the region of small χ^2 , this function exhibits similar general features as that used in our previous global fits [10], while it does not suffer from numerical instabilities arising from multiple minima. The two functions deviate at large values of χ^2 , where in any case poor fits result.

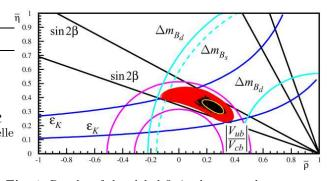


Fig. 1. Results of the global fit in the $\bar{\rho} - \bar{\eta}$ plane.

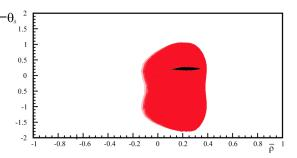


Fig. 2. Fit results in $\theta_s - \bar{\rho}$ plane from $a_{\phi K_0^0}$.

Table 3. Results of 95% C.L. range for $\bar{\rho}, \bar{\eta}, \alpha$ and γ from the global fits shown in figure 1. For comparison results from RFIT and the Bayesian method are also given.

parameter	Scan method	RFIT [9]	Bayesian [9]
$ar{ ho}$	-0.13 to 0.40	0.091 to 0.317	0.137 - 0.295
$ar{ar{\eta}}$	0.22 to 0.48	0.273 to 0.408	0.295 - 0.409
α	50.4° to 126.6°		
γ	34.4° to 91.7°	42.1° to 75.7°	47.0° to 70.0°

3 Results of the global Fit

Figure 1 shows the result of scanning all T_i simultaneously within $\pm 1\Delta$ of their allowed range except for the QCD parameters. We have used the input measurements summarized in table 1 and ranges for the T_i listed in table 2. The black points represent the best estimates of $(\bar{\rho}, \bar{\eta})$ for each model that is consistent with the data. The grey region shows the overlay of all corresponding 95% C.L. $\bar{\rho} - \bar{\eta}$ contours. For reference, the light ellipse depicts a typical contour. To guide the eye the 95% C.L. bounds on $|V_{ub}/V_{cb}|$, $|\epsilon_K|$, Δm_{B_d} and $\sin 2\beta$ as well as the lower bound on Δm_{B_s} are also plotted. From these fits we derive 95% C.L. ranges for $\bar{\rho}, \bar{\eta}, \alpha$ and γ that are listed in table 3. For comparison, recent results from two other global fits (RFIT [4], Bayesian fit [3]) are also shown.

Using the same source of inputs, several differences exist between the scan method and the other two approaches. First, we scan separately over the inputs of exclusive and inclusive $b \to u\ell\nu$ and $b \to c\ell\nu$ measurements. Second, we use a different approach to incorporate Δm_{B_s} . While in the Bayesian method theoretical quantities are parameterized in terms of gaussian and uniform distribu-

tions, we make no assumptions about their shape. Thus, the Bayesian fits tend to produce a smaller region in the $\bar{\rho}-\bar{\eta}$ plane and are more sensitive to fluctuations than corresponding fits in the scan method. In RFIT, the $\bar{\rho}-\bar{\eta}$ plane is scanned to find a solution in the theoretical parameter space. Since in RFIT a central region with equal likelihood is determined, it is not possible to give probabilities for individual points. In contrast, in the scan method individual contours have a statistical meaning, with the center point yielding the highest probability. Since the mapping of the theory parameters to the $\bar{\rho}-\bar{\eta}$ plane is not one-to-one, it is possible in the scan method to track which values of $(\bar{\rho},\bar{\eta})$ are preferred by the theory parameters.

4 Search for New Physics

The decay $B \to \phi K_S^0$ that proceeds via a $b \to s\bar{s}s$ penguin loop is expected measure $\sin 2\beta$ in the SM to within $\sim 4\%$. New physics contributions, however, may introduce a new phase θ_s that may change the CP asymmetry $a_{\phi K_S^0}$ significantly from $a_{J/\psi K_S^0}$. The BABAR/Belle average of $S_{\phi K_S^0} = -0.39 \pm 0.41$ has been updated this summer yielding $S_{\phi K_S^0} = -0.14 \pm 0.33$ [11]. The deviation from $\sin 2\beta$ has remained at $\sim 2.6\sigma$. In our global fit we introduce a new phase θ_s . Figure 2 shows the overlay of all resulting contours in the $\theta_s - \bar{\rho}$ plane that have acceptable fit probabilities. Presently, the phase is consistent with zero as expected in the SM.

Physics beyond the SM may affect $B_d^0 \bar{B}_d^0$ mixing and CP violation in $B \to J/\psi K_s^0$ and $B \to \pi\pi$. Using a model-independent analysis [12] we can introduce a scale parameter, r_d , for $B_d^0 \bar{B}_d^0$ mixing and an additional phase, θ_d , for parameterizing $a_{\psi K_s^0}$. In the SM we expect $r_d = 1$ and $\theta_d = 0$. With present uncertainties r_d and θ_d are consistent with the SM expectations (see [10]).

5 Visualizing the role of theoretical errors

In addition to the global fits in the $\bar{\rho} - \bar{\eta}$ plane, we explore the impact of measurements on the theoretical parameters and their correlations. We typically scan theory parameters within $\pm 5\Delta$ and denote them with \sim . Presently, we use either exclusive or inclusive \widetilde{V}_{ub} , \widetilde{V}_{cb} information and plot contours for three of the five scanned theoretical parameters for different conditions. An example is shown in Figure 3, where we have scanned inclusive V_{ub} , inclusive \widetilde{V}_{cb} , \widetilde{B}_K , $f_{B_d}\sqrt{B_{B_d}}$ and $\widetilde{\xi}$. For \widetilde{V}_{ub} , \widetilde{V}_{cb} and \widetilde{B}_K we plot two-dimensional contours on the surface of a cube. In each plane five contours are visible. The outermost contour (solid black) results from requiring a fit probability of > 32%. The next contour (also solid black) is obtained by restricting all other undisplayed theory parameters to their allowed range of $\pm 1\Delta$. The third solid line results by fixing the parameter orthogonal to plane to the allowed range, while the outer dashed line is found if the latter parameter is fixed to its central value. The internal dashed black line is obtained by fixing all undisplayed

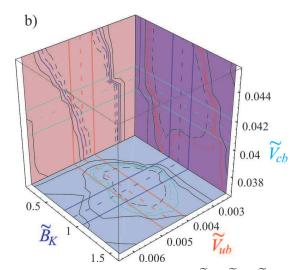


Fig. 3. Contours of the theory parameters $\widetilde{B}_K - \widetilde{V}_{ub} - \widetilde{V}_{cb}$ both resulting from inclusive reduced semileptonic rates for fit probabilities $P(\chi^2) > 32\%$ after scanning $\widetilde{B}_K, \widetilde{f}_B \sqrt{B_B}, \widetilde{\xi}, \widetilde{\Gamma}(B \to X_c \ell \nu)$ and $\widetilde{\Gamma}(B \to X_u \ell \nu)$ over $\pm 5\Delta_i$ range.

parameters to their central values. Further details, other combination plots and results for exclusive \tilde{V}_{ub} and \tilde{V}_{cb} scans are discussed in [10].

6 Conclusion

The scan method provides a conservative, robust method that treats non-gaussian theoretical uncertainties in an unbiased way. This reduces conflicts with the SM resulting from unwarranted assumptions concerning the theoretical uncertainties, which is important in searches for new physics. The scan methods yields significantly larger ranges for the $\bar{\rho}-\bar{\eta}$ plane than the Bayesian method. Presently, all measurements are consistent with the SM expectation due to the large theoretical uncertainties. The deviation of $a_{\phi K_s^0}$ from $\sin 2\beta$ measured in charmonium $K_S^0(K_L^0)$ modes is interesting but not yet significant. Modelindependent parameterizations will become important in the future when theory errors are further reduced.

References

- 1. L. Wolfenstein, Phys. Rev. Lett. **51** (1983) 1945.
- BABAR collaboration (P.F. Harrison and H.R. Quinn, eds.) SLAC-R-0504 (1998).
- 3. M. Ciuchini et al., J. High Energy Physics 107 (2001) 13.
- 4. A. Höcker et al., Eur. Phys. J. C 21 (2001) 225.
- 5. K. Schubert, CKM workshop Durham, April 5-9 (2003).
- 6. K. Hagiwara et al., Phys. Rev D 66 (2002) 010001.
- 7. D.E. Groom et al., Eur. Phys. J. C15 (2000) 1.
- 8. M.P. Jimack et al., Nucl. Instr. Meth. A408, (1998) 36.
- 9. M. Battaglia et al., hep-ph/0304132 (2002).
- 10. G.P. Dubois-Felsmann et al., hep-ph/0308262 (2003).
- 11. http://www.slac.stanford.edu/xorg/hfag/.
- 12. Y. Grossman et al. Phys.Lett. **B407** (1997) 307.